13th ewtec 2019 Proceedings of the 13th European Wave and Tidal Energy Conference 1-6 Sept 2019, Naples, Italy

A novel point absorber wave energy harvester with a Scotch Yoke mechanism

Elie Al Shami, Xu Wang, Zhenwei Liu

Abstract—**Wave energy harvesters (WECs) and especially point absorbers are very theoretically mature, but only a handful of devices were tested at full scale levels and there is very limited commercial development. There are many reasons for the retardation of industrial development; one of which is the difficulties for testing at full scale levels because of the harsh ocean wave environment, and another one is that most of the Power Take Off (PTO) techniques used with WECs are linear generators, which are very expensive to develop and manufacture. Therefore, this paper suggests a novel PTO concept, based on the Scotch Yoke mechanism where the harmonic linear motion of the buoy is converted to the rotary motion of a shaft connected to an off the shelf generator. The mechanism is designed to operate with a point absorber WEC. The equations describing the linear to rotary mechanism are incorporated with a hydrodynamic model and solved. Ansys Aqwa is used to simulate the hydrodynamic properties, and MATLAB is utilized to solve the full dynamic equations. The novel WEC PTO device with a Scotch Yoke mechanism is compared to the WEC PTO device with a crank slider mechanism which has already been developed and studied in the literature. The results indicate advantage of Scotch Yoke mechanism over a traditional crank slider mechanism for less maintenance requirements.**

Keywords— **point absorber, power take off, Scotch Yoke, wave energy converter.**

I. INTRODUCTION

THERE has been a lot of focus on renewable energy technologies lately, as most of the power grids around the world are slowly being connected to sustainable systems instead of the traditional fossil fuels based systems. Ocean waves energy harvesting has been in development since the late eighteen hundreds [1]-[2], and it's very conceptually interesting as the energy contained within ocean waves is around 5 times more dense than the energy in the wind [3]. Even though there has been a lot of research and development to optimize wave energy harvesters, only a handful of devices have reached the real ocean testing stage [4]-[8], and the ocean waves energy harvesting technology still didn't achieve a breakthrough in industrial development and commercialization [9].

There are two main reasons for the retardation of ocean waves energy harvesters development. The first one being the difficulties imposed by the harsh ocean environment testing, especially considering that most of the devices rely on resonance to absorb a reasonable amount of power [10]-[12]. This translates to the necessity of designing massive structures, and hence complicated linear generators which are able to resonate with the low frequency of ocean waves [13]. Such large structures are expensive to manufacture, transport, and install in an offshore location, where the environmental conditions are far from ideal. The second difficulty is the PTO (Power Take Off). Ideally, permanent magnet linear generators suit WECs as the ocean conditions impose low velocities because of the low ocean waves frequencies and high wave excitation forces. The issue of these linear generators is that they are expensive and are usually very large in dimensions in order to absorb a reasonable amount of energy [14]-[16]. The high cost of PTO research and development, and the difficulties surrounding real ocean experiments because of the large dimensions required are two main obstacles that researchers are attempting to overcome.

Rhinefrank, et al. [17] compared 18 different PTO mechanisms which suit the purpose of ocean waves energy harvesting. It was found that linear to rotary mechanisms, connected to a buoy from one end, and a rotary synchronous generator from the other end are a potential candidate for harvesting ocean wave energy, even in high energetic locations. These mechanisms might not be as ideal as permanent magnets linear generators, but they offer benefits that can help wave energy harvesters to overcome the obstacles showcased earlier. These mechanisms are technologically mature and well optimized, they can also be connected to off-the shelf rotary generators, rendering their manufacturing cost

ID number: 1289. Wave device development and testing.

E. Al Shami is a PhD candidate at RMIT university working on ocean waves energy harvesting. School of Engineering, RMIT University, Australia. (e-mail: elie.shami@rmit.edu.au).

X. Wang is a professor at RMIT university working on harvesting energy from vibrations and oscillating systems. School of Engineering, RMIT University, Australia. (e-mail: xu.wang@rmit.edu.au).

Z. Liu is a PhD candidate at RMIT university working on ocean waves energy harvesting. School of Engineering, RMIT University, Australia. (e-mail: s3500402@student.rmit.edu.au).

very cheap. Even though these mechanisms would generate more power with resonance due to the increase of velocities, they can potentially absorb a reasonable amount of power in normal conditions, given that a large gearbox is providing enough rotational velocity to the generator. This translates to the possibility of connecting these PTOs to small buoys, making real ocean testing and development cost effective and interesting for commercialization.

There have been more than one proposal of linear to rotary mechanisms designed for ocean waves energy harvesting. Liang, et al. [8] used a rack and pinion mechanism within a motion rectifying system to transform the up and down heave oscillations of the buoy into a unidirectional rotation of a generator's shaft. The simulation results matched well with the lab and real sea testing, and it was found that this system requires less optimal damping then an equivalent linear generator, resulting in lower PTO forces and an increase in the robustness of the system. Also, the proposed concept was able to harvest more power than an equivalent linear generator system in the simulations. Another novel linear to rotary concept was designed by De Koker, et al. [18]. The concept utilizes a planetary gears system connected to three shafts to ensure both linear to rotary transmission and control. The advantage of the system is that it was modelled to ensure that the generator is always rotating at the rated speed, resulting in a system efficiency of 88%. It should be noted that this efficiency excludes the power used to control the system.

Some proposed mechanisms were able to transform both the heave and roll/pitch motions into the rotation of a generator and were also sealed within a spherical buoy. Boren, et al. [19] used a vertical axis pendulum which rotates a generator. The PTO was parametrically studied with both simulations and scaled-down experiments. A similar PTO was proposed by Takaramoto, et al. [20], where a spherical ball gliding around the edges of the buoy rotates a generator placed at the middle, via a rope connection. The device was mathematically modelled with both a fixed damping and a controlled system.

Other mechanisms utilize pulleys to transfer the linear motion into rotary one. Dai, et al. [21] designed a pulley sealed inside a buoy, and connected via a rope to a submerged body, utilizing the relative movement between the two bodies to rotate the pulley. The rotating shaft has a spring on one end to store the excess energy, and a gearbox/generator on the other end. 20% efficiency was achieved with a scaled down model tested in a wave tank. Another concept which uses pulleys was proposed by Hadano, et al. [22]. The first iteration relied on a counterweight connected to the buoy via 2 pulleys which transformed the heave motion into the rotation of a shaft connected to a gear/ratchet system and a generator. The second iteration removed the counterweight and introduced a closed loop system with 4 pulleys. The second iteration was proved to increase the efficiency and lower the tension in the cables with simulations and wave tank experiments.

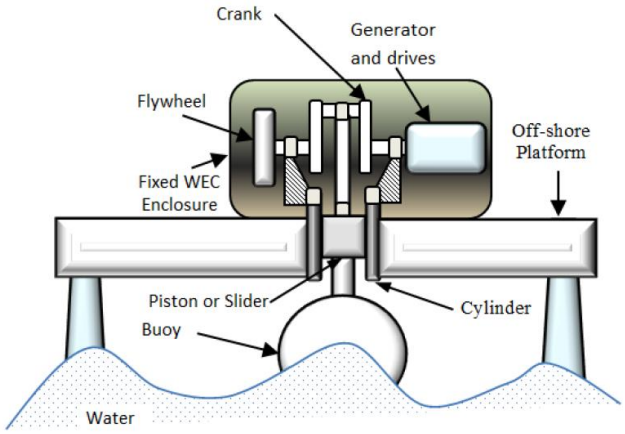

Fig. 1. Crank slider PTO [23]-[24].

One promising concept of a linear to rotary transfer mechanism is the crank slider mechanism, similar to an internal combustion engine mechanism. Sang, et al. [23] modelled such a crank slider mechanism as seen in Figure 1 and applied it to wave energy harvesting with a control algorithm to ensure resonance under the excitation of regular waves. Then the same mechanism was modelled in the time domain under the excitation of irregular waves in [24]. In both conditions, the control algorithm ensured that the electrical impedance matches the hydrodynamic one to increase the power capture. The simulations showcased that the device is able to capture a good amount of power, even in irregular waves, and a changeable gear ratio would stabilize and increase the power capture. Even with a flywheel, the rotational velocity of the generator shaft was not stable or constant as shown in figure 2 below.

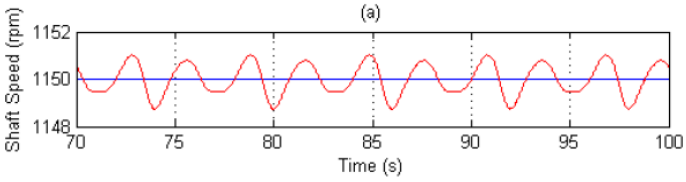

Fig. 2. Generator shaft rotational velocity, connected to a crank slider mechanism PTO [23].

This instability of the rotational velocity of the system's shaft will generate a lot of fatigue on the WEC, and being an offshore mechanism, where maintenance is difficult, this creates a dent in the structural integrity and robustness of this concept. Also the output voltage will suffer from the same fluctuations, indicating the need for more power electronic devices to smooth out the output. This instability is caused by the fact that the crank slider mechanism is not harmonic, while it's being excited by harmonic ocean waves' forces.

This paper suggests using a scotch yoke mechanism [25] to transfer the linear up and down heave oscillation of the buoy into one directional rotation of a generator. The scotch yoke mechanism is simpler than the crank

slider, with less moving parts, and more importantly it's a harmonic mechanism, matching with the harmonic ocean waves excitation. Even irregular waves are a superposition of harmonic waves. This might not translate to generating more power compared to a crank-slider mechanism, but it will result in a simpler mechanism, with less moving ports, less fatigue on the system, and a constant generator shaft velocity.

The rest of the paper introduces the mathematical model of both the scotch yoke and crank slider mechanisms connected to the same heaving buoy and generator, then results and discussion will be presented, the shortcomings of the design and possible solutions are discussed and finally some conclusions will be drawn.

II. MATHEMATICAL FORMULAE

A. Hydrodynamic buoy model

In the first section of the mathematical model, the hydrodynamic modelling of the buoy will be introduced. The buoy is locked in heave by the mechanism. The PTO resistive force on the buoy is assumed to be a linear damping force, given that the generator is an off the shelf DC or synchronous AC generator. The equation of motion is based on the Newton's second law, and incorporation of the linear potential flow theory where the flow is assumed to be irrotational and incompressible [11, 12]:

$$M\ddot{y} + C\dot{y} + Ky = F_{wave} - F_{PTO} - F_{viscous\ drag} \quad (1)$$

where y is the heave displacement of the buoy. M is total mass of the buoy and is composed of the physical dry mass m_d and hydrodynamic added mass m_a. The buoy must maintain neutral buoyancy and its dry mass is equal to the buoyancy force exerted on its submerged volume, which is the weight of the displaced volume of water: $m_d = \pi . {r_b}^2 . s_h . \rho$ where r_b is the radius of the buoy, s_h is its submerged height or draft, and ρ is the density of water. C is the linear hydrodynamic damping coefficient on the buoy, and is composed of mostly the hydrodynamic radiation damping coefficient c_r. The PTO resistive force is F_{pto}. $F_{viscous\ drag}$ is the viscous damping force opposing the movement of the buoy. K is the total stiffness acting on the buoy, and since the PTO mechanism doesn't include any springs or reaction forces, this term is composed of only the hydrostatic stiffness k_h which is resulted from the difference between the weight of the buoy and its buoyancy while oscillating, and can be calculated by: $k_h = \pi . {r_b}^2 . \rho . g$ where g is the gravitational acceleration. F_{wave} is the wave excitation force exerted on the buoy.

The hydrodynamic terms arise from the linear potential flow theory. The wave excitation force term is derived from integrating the pressure of the incident wave over the surface area of the buoy. The other hydrodynamic terms are derived from integrating the radiated wave pressure over the surface area of the buoy, which results in a hydrodynamic added mass term proportional to the acceleration of the buoy, and a radiation damping term proportional to its velocity.

One can also utilize the time domain to solve equation (1) where nonlinearities and accurate wave/buoy interactions can be incorporated into the model [26]. In the time domain, the Cummins equation is utilized [27]:

$$(m_d + {m_a}^{\infty})\ddot{y}_{(t)} + \int_{-\infty}^{t} RIF(t-\tau)\dot{y_{(t)}} d\tau + k_h y_{(t)} = F_{wave(t)} - F_{PTO(t)} - F_{viscous\ drag(t)} \quad (2)$$

where $y_{(t)}$, $\dot{y_{(t)}}$, and $\ddot{y}_{(t)}$ are the instantaneous displacement, velocity and acceleration of the buoy in the heave direction respectively. ${m_a}^{\infty}$ is the hydrodynamic added mass of the buoy at the infinite frequency. The second term of equation (7) is the convolution integral of the impulse function. This term represents the radiation effects in the time domain where RIF is the Radiation Impulse Function and it is the reverse Fourier transform of the frequency dependent radiation damping coefficient c_r from the frequency domain to the time domain. The incoming wave is modeled as a regular wave, and $F_{wave(t)}$ can be calculated as follows [28]:

$$F_{wave(t)} = A . f_e . \sin(wt + \emptyset) \quad (3)$$

where f_e and $\emptyset$ are the frequency dependent magnitude and phase of the wave excitation force respectively. These entities, along with the added mass m_a and radiation damping coefficient c_r can be calculated using a BEM (Boundary Element Method) simulation in Ansys Aqwa. ω is the wave frequency in *rad/s* and A is the wave height.

The PTO resistive force on the system is assumed linear [8] and is of the form:

$$F_{pto} = c_p . \dot{y_{(t)}} \quad (4)$$

where c_p is the linear PTO damping coefficient.

The viscous damping drag force is non-linear and is modeled as the Morison drag force:

$$F_{viscous\ drag(t)} = \frac{1}{2} . \rho . c_d . s_a . {\dot{y_{(t)}}}^2 \quad (5)$$

where s_a is the cross sectional surface area of the heaving buoy, and c_d is the non-dimensional viscous drag coefficient and is usual a unity for cylinders [29, 30].

B. Crank slider model

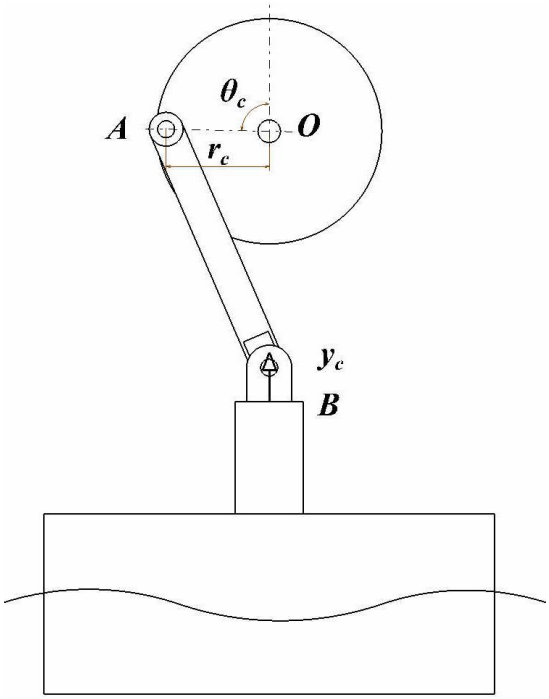

Fig. 3. Schematic of the crank slider mechanism connected to a buoy.

Fig. 3 shows a schematic of the crank slider, with θ_c being the crank angle between the short link and the vertical, and $y_{c(t)}$ is the instantaneous vertical displacement of joint B. r_c is the radius of the flywheel (OA). l is the length of the long link. The vertical heaving oscillation of the buoy pushes joint B like an engine's piston, rotating joint A around the center of the flywheel O. They buoy and the piston are rigidly connected; hence $y_{c(t)} = y_{(t)}$ and $y_{(t)} = 0$ corresponds to the buoy at the surface of the water, not excited by any wave, resulting in $\theta_c = {}^{\pi}/_{2}\ rad.$

The geometric relation, linking the instantaneous crank angle to the piston's displacement is:

$$y_{c(t)} = d - r_c.\cos\left(\theta_{c(t)}\right) - \sqrt{l^2 - \left(r_c.\sin\left(\theta_{c(t)}\right)\right)^2} \tag{6}$$

Performing mathematical operations on equation (6), renders the following solution for the crank angle:

$$\theta_{c(t)} = \cos^{-1}\left(\frac{l^2-\left(y_{c(t)}-d\right)^2-{r_c}^2}{2.r_c.\left(y_{c(t)}-d\right)}\right) \tag{7}$$

Performing derivation with respect to time on $\theta_{c(t)}$ in equation (7) will result in calculating the instantaneous velocity and acceleration of the shaft, $\dot{\theta_{c(t)}}$ and $\ddot{\theta_{c(t)}}$ respectively.

The driving torque for the crank-slider mechanism, connected to a heaving buoy is the link between the oscillating floater and the PTO mechanism and is calculated as follows:

$$T_{dc(t)} = F_{pto(t)}.r_c.\sin\left(\theta_{c(t)}\right).\left[1 + \frac{\frac{r_c}{l}.\cos(\theta_{c(t)})}{\sqrt{\left(1-\left(\frac{r_c}{l}\sin(\theta_{c(t)})\right)^2\right)}}\right] = c_p.\dot{y_{(t)}}.\ r_c.\sin\left(\theta_{c(t)}\right).\left[1 + \frac{\frac{r_c}{l}.\cos(\theta_{c(t)})}{\sqrt{\left(1-\left(\frac{r_c}{l}\sin(\theta_{c(t)})\right)^2\right)}}\right] \tag{8}$$

C. Scotch Yoke model

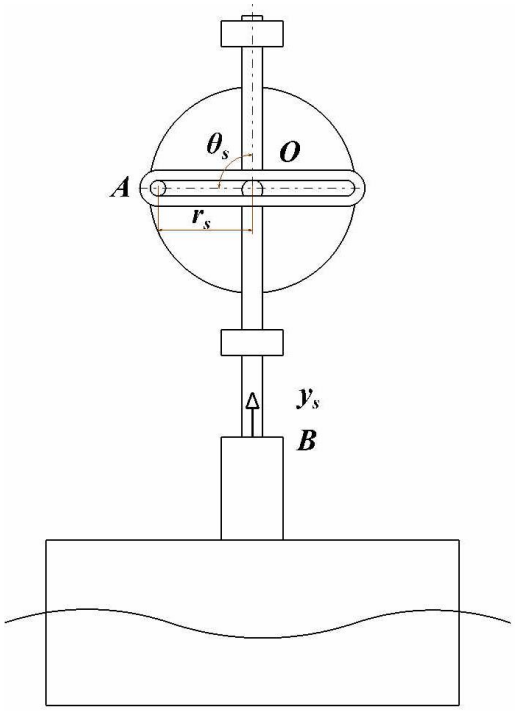

Fig. 4. Schematic of the Scotch Yoke mechanism connected to a buoy.

Fig. 4 shows a schematic of the Scotch Yoke, with θ_s being the angle between OA and the vertical, and $y_{s(t)}$ is the instantaneous vertical displacement of point B. r_s is the radius of the flywheel (OA). The vertical heaving oscillation of the buoy pushes the yoke upwards and downwards similar to an engine's piston, rotating the bearing at point A around the center of the flywheel O. The buoy and the piston are rigidly connected; hence $y_{s(t)} = y_{(t)}$ and $y_{s(t)} = 0$ corresponds to the buoy at the surface of the water, not excited by any wave, and yielding $\theta_s = {}^{\pi}/_{2}\,rad.$

The geometric relation, linking the instantaneous angle of rotation $\theta_{s(t)}$ to the piston's displacement is:

$$\theta_{s(t)} = \cos^{-1}\left(\frac{y_{s(t)}}{r_s}\right) \tag{9}$$

Performing derivation with respect to time on $\theta_{s(t)}$ in equation (9) will result in calculating the velocity and acceleration of the shaft, $\dot{\theta}_{s(t)}$ and $\ddot{\theta}_{s(t)}$ respectively.

The driving torque for the Scotch Yoke mechanism, connected to a heaving buoy is the link between the oscillating floater and the PTO mechanism and is calculated as follows:

$$T_{ds(t)} = F_{pto(t)}.r_s.\sin(\theta_{s(t)}) = c_p.\dot{y_{(t)}}.r_s.\sin(\theta_{s(t)}) \tag{10}$$

D. Power calculation

Both the crank-slider and the Scotch Yoke are modelled to be connected to same buoy from one end, and to the same shaft/gearbox/generator from the other end, similarly to Fig. 1. The procedure of the power calculation will be the same for both models. Applying the summation of moments around the rotating shaft yields:

$$T_{drive} - T_{gen} = (\sum j).\ddot{\theta} \quad (11)$$

T_{drive} is the drive torque provided by the heaving buoy, T_{gen} is the torque of the generator, $\ddot{\theta}$ is the rotational acceleration of the shaft, and $\sum j$ is the summation of the moments of inertias of the different components (shaft, gearbox, motor…).

The instantaneous generated power is:

$$P_{(t)} = \frac{T_{gen(t)}}{N}.\dot{\theta}_{(t)}.N = T_{gen(t)}.\dot{\theta}_{(t)} \quad (12)$$

where N is the gearbox ratio. To calculate the instantaneous power output of the crank slider model, equations (8) and (11) can be plugged into equation (12):

$$P_{Crank\ slider(t)} = \left(T_{dc(t)} - (\sum j).\ddot{\theta_{c(t)}}\right).\dot{\theta}_{c(t)} = \left(c_p.\dot{y_{(t)}}.\ r_c.\sin(\theta_{c(t)}).[1 + \frac{\frac{r_c}{l}.\cos(\theta_{c(t)})}{\sqrt{(1-(\frac{r_c}{l}\sin(\theta_{c(t)}))^2)}}] - (\sum j).\ddot{\theta_{c(t)}}\right).\dot{\theta}_{c(t)} \quad (13)$$

To calculate the instantaneous power output of the scotch yoke model, equations (10) and (11) are plugged into equation (12):

$$P_{Scotch\ yoke(t)} = \left(T_{ds(t)} - (\sum j).\ddot{\theta_{(t)}}\right).\dot{\theta}_{s(t)} = \left(c_p.\dot{y_{(t)}}.r_s.\sin(\theta_{s(t)}) - (\sum j).\ddot{\theta_{s(t)}}\right).\dot{\theta}_{s(t)} \quad (14)$$

And the average power output is calculated with the following integration:

$$\bar{P} = \frac{1}{T}\int_0^t P_{(t)}dt \quad (15)$$

For the Crank slider model, the average power output over a period T is:

$$\overline{P_{Crank\ slider}} = \frac{1}{T}\int_0^t \left(c_p.\dot{y_{(t)}}.\ r_c.\sin(\theta_{c(t)}).[1 + \frac{\frac{r_c}{l}.\cos(\theta_{c(t)})}{\sqrt{(1-(\frac{r_c}{l}\sin(\theta_{c(t)}))^2)}}] - (\sum j).\ddot{\theta_{c(t)}}\right).\dot{\theta}_{c(t)}dt \quad (16)$$

And finally, for the Scotch yoke model, the average power output over a period T is:

$$\overline{P_{Scotch\ yoke}} = \frac{1}{T}\int_0^t \left(c_p.\dot{y_{(t)}}.r_s.\sin(\theta_{s(t)}) - (\sum j).\ddot{\theta_{s(t)}}\right).\dot{\theta}_{s(t)}dt \quad (17)$$

The incident wave power is defined as [31]:

$$P_{wave} = \rho.g.A^2.r_b.\frac{\lambda}{T_w} + \frac{2.\pi.g.A^2.d_o.r_b}{T_w.\cosh(4.\pi.d_o/\lambda)} \quad (18)$$

where λ is the wavelength, T_w is the period of the incident wave, and d_o is the ocean depth.

The efficiency of the scotch yoke mechanism is calculated as follows:

$$\eta_{Scotch\ yoke} = \frac{\overline{P_{Scotch\ yoke}}}{P_{wave}} \quad (19)$$

III. RESULTS AND DISCUSSION

This section will provide the preliminary results of the previous mathematical model to introduce the scotch yoke mechanism and then compare the crank slider to the Scotch Yoke. Both PTOs are connected to the same cylindrical heaving buoy, and its parameters are displayed in Table I.

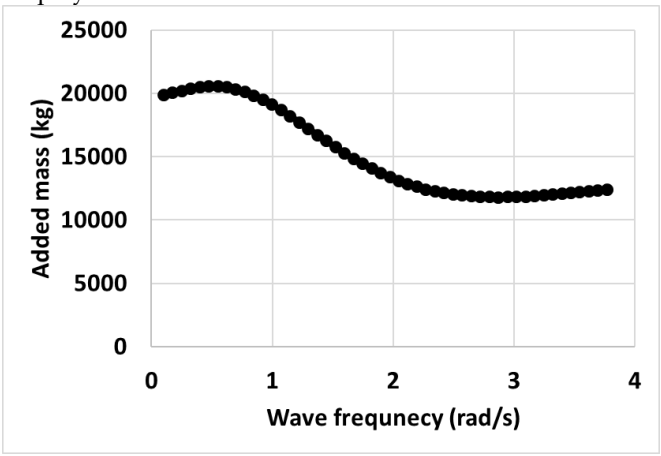

Fig. 5. Buoy's added mass vs incoming wave frequency.

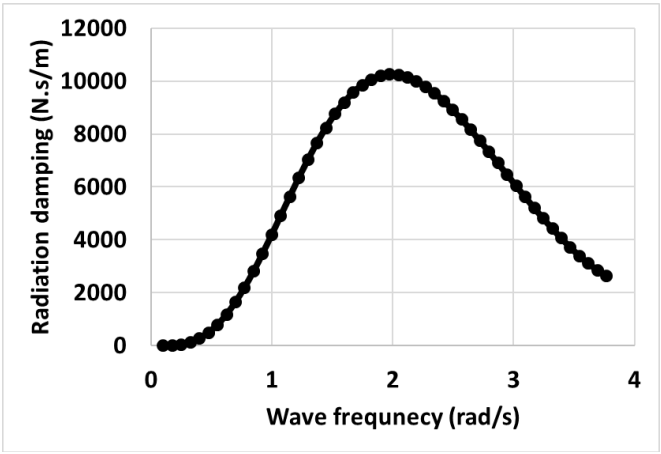

Fig. 6. Buoy's radiation damping vs incoming wave frequency.

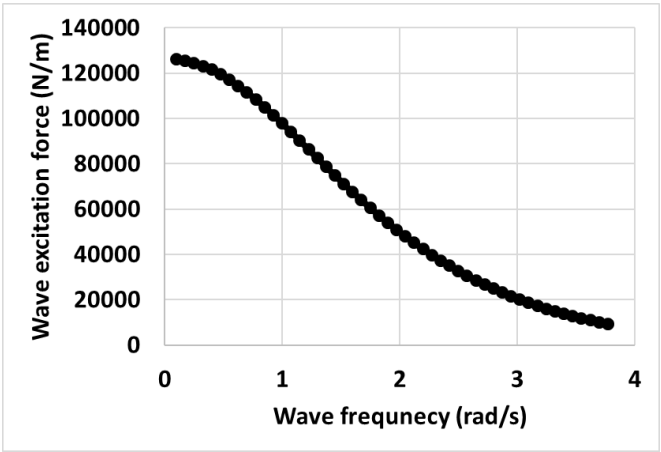

Fig. 7. Buoy's wave excitation force vs incoming wave frequency.

The frequency dependent hydrodynamic coefficients of the buoy are calculated using a simulation in Ansys Aqwa and are shown in Figs 5-7.

It should be noted that this work is part of a project dedicated to developing ocean waves energy harvesting for Australia. The studied devices will be placed offshore and the targeted wave height is 1m, while the targeted wave period is 8 s [13], [32], [33]. The physical parameters of the scotch yoke mechanism are shown in Table II, while the physical parameters of the crank slider mechanism are shown in Table III.

To determine the optimal PTO damping of the system, we must determine the maximum value of PTO damping that ensures that the heave amplitude of the buoy is 1m so that the mechanism achieves a full rotation without the assistance of the flywheel. As stated earlier, the wave height and period values are 1 m and 8 s respectively. Fig. 8 below displays the heave amplitude of the buoy vs. the PTO damping coefficient of the scotch yoke system for the targeted sea state. The maximum value of PTO damping that ensures a buoy heave amplitude of 1m, and therefore a full rotation cycle of the scotch yoke mechanism is 11270 N.s/m.

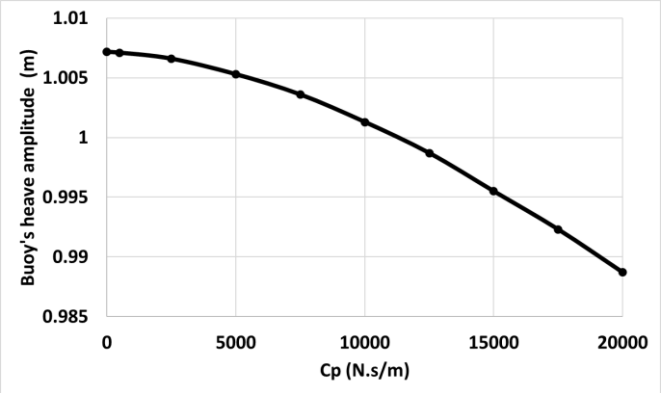

Fig. 8. The heave amplitude of the buoy vs the PTO damping coefficient of the scotch yoke mechanism. Wave height= 1m and wave period =8s.

The average absorbed power from equation (17) is plotted against different PTO damping values from 0 to 11270 N.s/m for the scotch yoke mechanism in Fig. 9. It should be noted that the peak torque value provided to the generator is displayed on the right-hand side vertical axes. The absorbed average power seems to linearly increase with the PTO damping coefficient for this sea state, and the PTO damping value that resulted in the maximum average absorbed power at this wave height and period is 11270 N.m/s with a maximum value of 3404 W of average absorbed power, and a peak torque provided to the generator of 88 N.m. It should be noted that a higher PTO damping value would result in an increase in the torque provided at the generator shaft, and hence more power. But a high damping value will result in damped buoy oscillation, hence the mechanism would have to rely on the flywheel to complete a full rotation, and the purpose of this work is to focus on the scotch yoke linear to rotary mechanism itself, and its operation as a part of a WEC PTO.

To observe how the absorbed power of the scotch yoke mechanism changes with different wave frequencies and PTO damping values, the average power from equation (17) is plotted for different linear PTO values vs the incident wave frequencies in Fig. 10.

TABLE I
BUOY AND WAVE PARAMETERS

Wave height	1 m
Target wave period	8 s
Water density	1025 kg/m^3
Gravitational acceleration	9.81 m/s^2
Buoy radius	2 m
Buoy height	1.6 m
Buoy draft	0.8m

TABLE II
SCOTCH YOKE PARAMETERS

Flywheel radius	1 m
Gearbox ratio	1:100
Link OA	1 m
Gearbox inertia	20 kg.m^2
Generator inertia	10 kg.m^2
Flywheel inertia	30 kg.m^2

TABLE III
BUOY AND WAVE PARAMETERS

Flywheel radius	1 m
Gearbox ratio	1:100
Link OA	1 m
Link AB	2.25 m
Gearbox inertia	20 kg.m^2
Generator inertia	10 kg.m^2
Flywheel inertia	30 kg.m^2

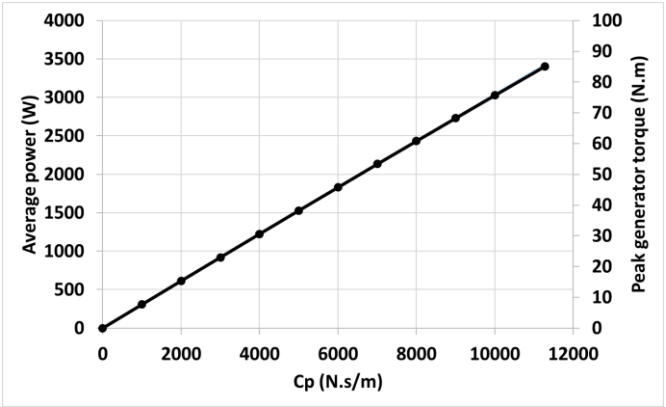

Fig. 9. The average absorbed power vs the PTO damping coefficient for the scotch yoke mechanism. Wave height= 1m and wave period =8s.

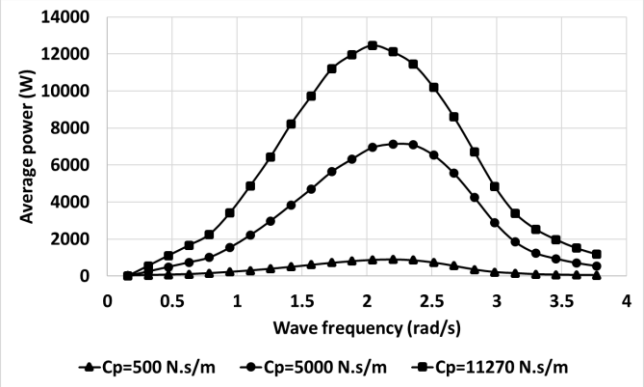

Fig. 10. The average absorbed power vs the incoming wave frequency for the scotch yoke mechanism with different PTO damping coefficients.

One can notice that the behavior is similar to other PTOs with a considerable increase in the captured power around resonance. This is due to the increase in the buoy heave velocity at resonance resulting in an increase of the shaft rotational velocity and hence an increase in the captured power. Also, for a constant PTO damping, the bandwidth of the device is considerably large for all PTO damping values. Finally, the captured power increased for all frequencies with the increase of the PTO damping, as the increase of damping for these cases increased the provided torque to the generator overcoming the velocity damping imposed by the higher PTO damping value.

For the rest of this section, the scotch yoke mechanism will be compared to the crank slider mechanism. Both PTOs are connected to the same buoy who's properties are displayed in Table I. The same linear PTO damping value of 11270 N.s/m was used for both models. Even though more power can be harvested at resonance, a wave period of 8s and wave height of 1m will be targeted with the buoy dimensions listed in table I. Optimizing the buoy dimensions to ensure resonance at this frequency will require very large dimensions, and the target here to compare two fairly sized models who can be subject for real testing. The gearbox ratio was chosen to be connected to a generator who's optimal performance is at 750 RPM. Fig. 11 showcases the buoy's heave response compared with the incident wave height for the first 3 periods of the simulation.

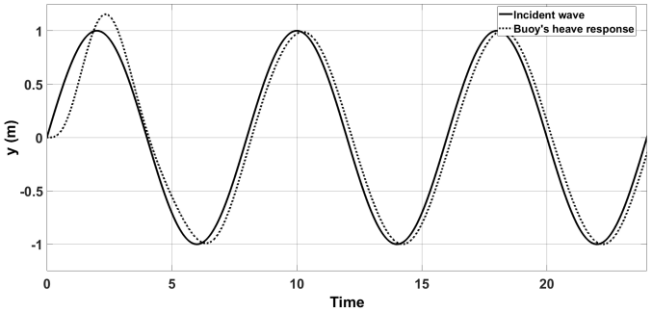

Fig. 11. First 3 periods of the buoy's heave oscillation compared with the incident wave height.

It should be noted that the phase difference between the incoming wave excitation force on the buoy and the incident wave is low for low frequencies. Also, the first period of the buoy's heave response should be disregarded as the solution hasn't converged yet.

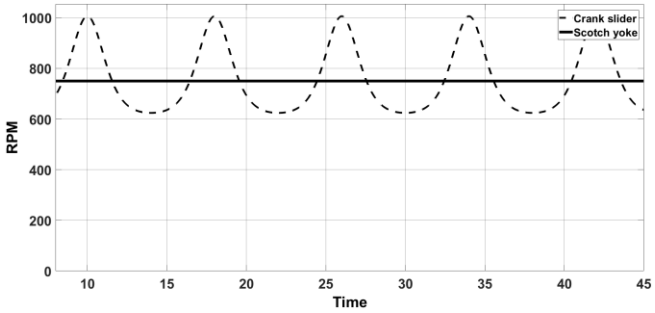

Fig. 12. The generator shaft RPM vs Time for both the Scotch yoke and the Crank slider mechanisms.

Fig. 12 compares the generator shaft rotational velocity in RPM of the Scotch yoke and the Crank slider mechanisms. The RPM of the shaft for the Scotch Yoke is constant at 750 RPM, while the RPM for the crank slider mechanism is fluctuating around that value, and this is somewhat consistent with Sang, et al. [23] as seen in Fig. 2. The reason for these fluctuations is the non-harmonic nature of the crank slider mechanism which result in unstable rotational velocities of the main shaft of the system when excited by purely harmonic ocean waves. On the other hand, the Scotch Yoke mechanism is harmonic by nature, resulting in a constant rotational velocity, as it is more compatible with the harmonic excitation with ocean waves. This will reduce the fatigue and loads on the system, which results in reducing the need for maintenance, also this will reduce the size of the flywheel, as the flywheel's only function in the scotch yoke mechanism is to assist with the top and low dead centers where the drive torque is null. Finally, the Scotch yoke mechanism presents a better grid connectivity, as the output voltage would be smoother since the velocity is constant, eliminating the need for electric rectifiers. Given that the rotational velocity of the Scotch Yoke's shaft is constant, this will result in nulling its acceleration, unlike the crank shaft's acceleration, as seen in the Fig. 13 below.

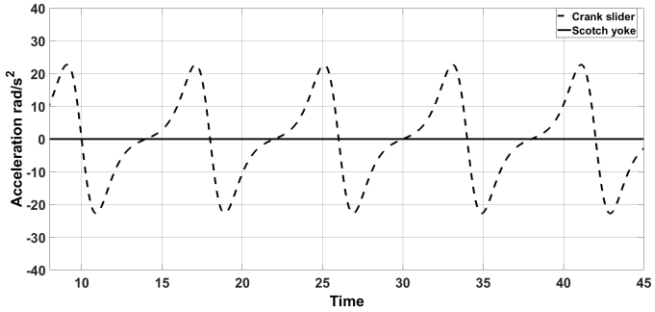

Fig. 13. The shaft rotational acceleration vs time for both the Scotch Yoke and the crank slider mechanisms.

The crank slider's shaft fluctuating rotational acceleration between +/-22.74 rad/s^2 will result in extra inertial forces on the PTO system compared to the Scotch yoke's zero rotational acceleration. This is also evident with the fluctuations of the drive torque as seen in Fig. 14, where the Scotch Yoke's drive torque is fluctuating harmonically between 0 N.m and 88.5 N.m, while the crank slider's drive torque has a different behavior, where it has two different repeating cycles, with one drive torque fluctuating between 0 N.m and 102 N.m and a another drive torque fluctuating between -3.7 N.m and 91 N.m. The reason for this is the effect of the gearbox, generator and flywheel's inertias from equation (11). Since the shaft's acceleration is not constant, these inertias will create loads on the system, resulting in fluctuating torques, which should compensate for the shaft's velocity fluctuations, and finally resulting in similar power output between the Scotch Yoke and the crank slider mechanisms. The absence of rotational acceleration and inertial loads in the Scotch Yoke mechanism lowers the effect of the flywheel on the power output, rendering the Scotch Yoke a cheaper and simpler solution for ocean waves energy harvesting.

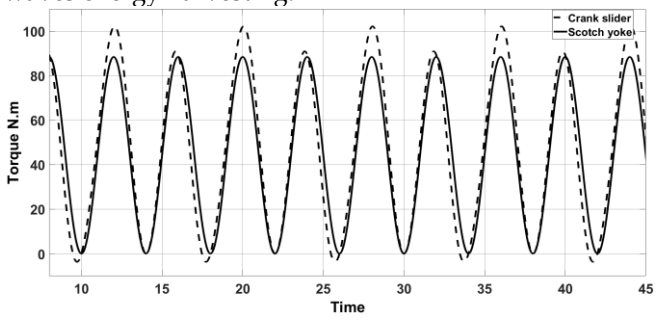

Fig. 14. The drive torque vs time for both the Scotch yoke and crank slider mechanisms.

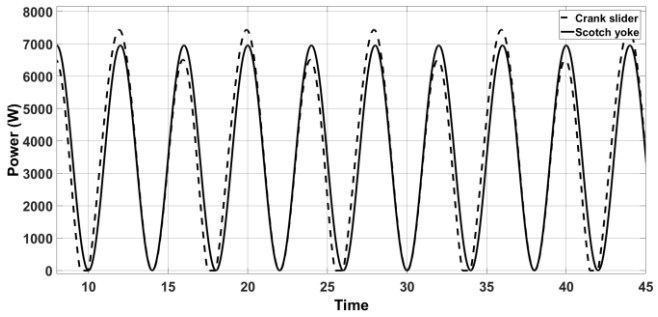

Fig. 15. The instantaneous power output vs time for both the Scotch Yoke and the crank slider mechanisms.

Fig. 15 displays the instantaneous power output from equations (13) and (14) of both the crank slider and Scotch Yoke PTO mechanisms connected to the same generator and heaving buoy. As predicted, the extra inertial loads from the flywheel, gearbox and generator caused by the rotational acceleration of the crank slider's shaft compensated for the rotational velocity fluctuation in the crank shaft PTO. This compensation resulted in similar power output between the crank slider and the Scotch Yoke mechanisms. the Scotch Yoke's instantaneous power fluctuated between 0 W and 6952 W, while the crank slider's instantaneous power output has two different repeating cycles, with one fluctuating between 0 W and 6510 W and another fluctuating between 0 W and 7434 W, with the difference being similar to the different behavior in the drive torque results. Even though this means that from equations (16) and (17) both systems ultimately produced the same average power of around 3500W over 50 seconds of simulation time, the power output of the Scotch Yoke mechanism is more harmonic, reducing the power electronics and control needed to have a proper smooth grid connectivity. Also, the efficiency of the Scotch yoke calculated from equation (19) is 28.5% for the simulated sea state, which is considerably high for a non-optimized WEC operating without resonance or control. The results will need further development, and the need for less power electronics to smooth out the output flow of the Scotch Yoke system will be validated when a generator is chosen, and both simulated and tested to check for the voltage output. Ultimately, both these designs present the same conceptual shortcomings, especially when it comes to the stroke length being equal to the wave height. Both designs absorbed the same amount of average power, but the scotch yoke proved to be a simpler more robust design for offshore wave energy harvesting.

IV. SHORTCOMINGS AND POSSIBLE SOLUTIONS

The proposed Scotch Yoke design was simulated and it is shown by the simulation results that it is more suitable than the crank slider mechanism for an offshore wave energy harvesting platform. But both mechanisms share the same problem, and that they both operate highly efficiently as long as the wave height is equal or close to the stroke length of the PTO mechanism, which is not the case for more realistic irregular ocean waves where the wave height is constantly changing. The flywheel inertia will help overcoming the difference between the wave height and the stroke length for low wave heights, and end stops would probably render the device more robust in case of very large wave heights. This problem isn't limited to the crank slider and Scotch Yoke mechanisms, even linear generators have an ideal stroke length, end stops, and an efficient usable area between the stator and the translator [14]-[16]-[34]-[35]. One possible solution would be to alter the mechanism to have a variable stroke translation to rotation motion conversion. This has been proposed before for the Scotch Yoke mechanism [36], and it will add more mechanical complexities to the system. Another solution will be implementing a control algorithm that works in a similar method to how the optimal damping was chosen in the previous section, with both the optimal power and damping the oscillation to the optimal amplitude in mind. The control resistive force will help keeping the oscillation damped so that the

heave amplitude is equal the Scotch yoke's stroke length. The problem with this solution is resonance, because of the high amplitudes and velocities of resonating heaving buoys, large resistive forces will be required to keep the devices heaving at the same amplitude as the scotch yoke's stroke length.

Also, to provide optimum rotational velocity to the generator with the variable periods of ocean waves a gearbox with a variable ratio might prove to be a proper workaround as suggested by Sang, et al. [24]. A planetary gearing system similar to the one proposed by De Koker, et al. [18] can be developed to tackle this issue.

Ultimately, the convenience of having a robust and relatively cheaper mechanism to harvest energy from ocean waves will come at the expense of the complexity of other components, such as the issue with the stroke length discussed earlier. The mechanism will also require end stops in case of large wave heights/forces, a well designed flywheel able to provide enough inertia to keep the mechanism running, and a robust and optimized gearbox to provide the required RPM to the generator. A 1:100 gearbox such as the one used in the mathematical model wouldn't be very easy to design and implement and would require a study on its own. Perhaps conducting a hydrodynamic optimization on the buoy and ensuring its operation in resonance would increase the velocities and hence reduce the necessity of a large gearbox.

Another shortcoming is the necessity of an already installed offshore platform to house the PTO and power electronics, as the device needs to be suitable for the installation on an oil platform for example [37]. The negativity of this would be that if a farm, or a large scale model are to be installed in an offshore location, a separate floater would be needed to support the weight of the PTO. A possible solution for this would be installing a heave plate to increase the heave stability of the device, and to support the weight of the PTO and power electronics, similarly to [5].

And finally, there is the issue of lubrication. The Scotch Yoke mechanism relies on the performance of the bearings to ensure smooth rotational motion. These bearings will need lubrication to keep the friction losses minimal. The solution for this would be to create an oil pumping system, powered by the heave motion of the buoy, to keep the bearing lubricated. This is similar to a traditional internal combustion engine, and the power needed to pump the oil would be very minimal compared to the power being harvested.

V. CONCLUSION

This paper introduced a new concept for a linear to rotary motion conversion mechanism to be installed in a PTO for a WEC. The concept should tackle some of the issues WECs are facing while also introducing some shortcomings that require more research to resolve. Even though it would operate more efficiently around resonance, the simulations showed an efficiency of 28.5% when the device isn't resonating with the incident waves, indicating an acceptable performance out of the resonance frequency. One of the biggest advantages of using linear to rotary motion transmission devices such as the Scotch yoke is that it is technologically mature, as it has been available for a long time. Additionally, it can be plugged into an off the shelf generator, unlike linear generators which still need more research development to be fully optimized for wave energy harvesting. And lastly, the device is simple, easy to maintain and relatively cheap, which could prove to be the step needed in ocean waves energy harvesting to push the technology towards more realistic sea testing and even commercialization.

The mathematical section showcased the modelling and simulation of the scotch yoke mechanism, its superiority to the crank slider counterpart, and its ability to have a smooth operation with 28.5% efficiency in non-resonating and uncontrolled conditions. The last section of the paper focused on some of the main issues and possible solutions. This PTO will be more optimized, and more work is being done to have it operate efficiently under different sea states, with a focus on irregular waves and the stroke length issue. Also, a scaled down model is being manufactured and will be tested in a wave tank to validate more simulations.

Fig. 16. 3d CAD drawing of the scaled down designed model.

ACKNOWLEDGEMENT

Authors would like thank Australia Research Council Discovery Project grant DP170101039 for financial support.

REFERENCES

[1] B. Drew, A. R. Plummer, and M. N. Sahinkaya, "A review of wave energy converter technology," *Proceedings of the Institution of Mechanical Engineers, Part A: Journal of Power and Energy,* vol. 223, no. 8, pp. 887-902, 2016.

[2] A. F. d. O. Falcão, "Wave energy utilization: A review of the technologies," *Renewable and Sustainable Energy Reviews,* vol. 14, no. 3, pp. 899-918, 2010.

[3] J. Falnes, *Ocean Waves and Oscillating Systems: Linear Interactions Including Wave-Energy Extraction*. Cambridge: Cambridge University Press, 2002.

[4] K. Rhinefrank, A. Schacher, J. Prudell, E. Hammagren, A. von Jouanne, and T. Brekken, "Scaled Development of a Novel Wave Energy Converter Through Wave Tank to Utility-Scale Laboratory Testing," (in English), *Ieee Pow Ener Soc Ge,* 2015.

[5] K. Rhinefrank *et al.*, "Development of a Novel 1:7 Scale Wave Energy Converter," (in English), *Omae2011: Proceedings of the Asme 30th International Conference on Ocean, Offshore and Arctic Engineering, Vol 5,* pp. 935-+, 2011.

[6] S. J. Beatty, M. Hall, B. J. Buckham, P. Wild, and B. Bocking, "Experimental and numerical comparisons of self-reacting point absorber wave energy converters in regular waves," *Ocean Engineering,* vol. 104, pp. 370-386, 2015.

[7] E. Lejerskog, C. Boström, L. Hai, R. Waters, and M. Leijon, "Experimental results on power absorption from a wave energy converter at the Lysekil wave energy research site," *Renewable Energy,* vol. 77, pp. 9-14, 2015.

[8] C. Liang, J. Ai, and L. Zuo, "Design, fabrication, simulation and testing of an ocean wave energy converter with mechanical motion rectifier," *Ocean Engineering,* vol. 136, pp. 190-200, 2017.

[9] K. Ruehl and D. Bull, "Wave Energy Development Roadmap: Design to Commercialization," (in English), *2012 Oceans,* 2012.

[10] J. Engström, V. Kurupath, J. Isberg, and M. Leijon, "A resonant two body system for a point absorbing wave energy converter with direct-driven linear generator," *Journal of Applied Physics,* vol. 110, no. 12, 2011.

[11] H. Yavuz, A. McCabe, G. Aggidis, and M. B. Widden, "Calculation of the performance of resonant wave energy converters in real seas," *Proceedings of the Institution of Mechanical Engineers, Part M: Journal of Engineering for the Maritime Environment,* vol. 220, no. 3, pp. 117-128, 2006.

[12] M. Eriksson, J. Isberg, and M. Leijon, "Hydrodynamic modelling of a direct drive wave energy converter," *International Journal of Engineering Science,* vol. 43, no. 17-18, pp. 1377-1387, 2005.

[13] J. Morim, N. Cartwright, A. Etemad-Shahidi, D. Strauss, and M. Hemer, "A review of wave energy estimates for nearshore shelf waters off Australia," *International Journal of Marine Energy,* vol. 7, pp. 57-70, 2014.

[14] L. Ulvgård, L. Sjökvist, M. Göteman, and M. Leijon, "Line Force and Damping at Full and Partial Stator Overlap in a Linear Generator for Wave Power," *Journal of Marine Science and Engineering,* vol. 4, no. 4, 2016.

[15] H. Polinder, M. E. C. Damen, and F. Gardner, "Design, modelling and test results of the AWS PM linear generator," *European Transactions on Electrical Power,* vol. 15, no. 3, pp. 245-256, 2005.

[16] H. Polinder, B. C. Mecrow, A. G. Jack, P. G. Dickinson, and M. A. Mueller, "Conventional and TFPM Linear Generators for Direct-Drive Wave Energy Conversion," *IEEE Transactions on Energy Conversion,* vol. 20, no. 2, pp. 260-267, 2005.

[17] K. Rhinefrank *et al.*, "Comparison of Direct-Drive Power Takeoff Systems for Ocean Wave Energy Applications," *IEEE Journal of Oceanic Engineering,* vol. 37, no. 1, pp. 35-44, 2012.

[18] K. L. De Koker *et al.*, "Modeling of a Power Sharing Transmission in a Wave Energy Converter," (in English), *2016 Ieee 16th International Conference on Environment and Electrical Engineering (Eeeic),* 2016.

[19] B. C. Boren, P. Lomonaco, B. A. Batten, and R. K. Paasch, "Design, Development, and Testing of a Scaled Vertical Axis Pendulum Wave Energy Converter," *IEEE Transactions on Sustainable Energy,* vol. 8, no. 1, pp. 155-163, 2017.

[20] R. Takaramoto, M. Kashiwagi, and K. Sakai, "Wave Energy Absorption in Irregular Waves by a Floating Body Equipped with Interior Rotating Electric-Power Generator," presented at the The Twenty-fourth International Ocean and Polar Engineering Conference, Busan, Korea, 2014/8/7/, 2014.

[21] Y. Dai, Y. Chen, and L. Xie, "A study on a novel two-body floating wave energy converter," *Ocean Engineering,* vol. 130, pp. 407-416, 2017.

[22] K. Hadano, K. Y. Lee, and B. Y. Moon, "A study on dynamic motion and wave power in multi-connected wave energy converter," *Ships and Offshore Structures,* vol. 11, no. 7, pp. 679-687, 2016.

[23] Y. R. Sang, H. B. Karayaka, Y. J. Yan, and J. Z. Zhang, "Resonance Control Strategy for A Slider Crank WEC Power Take-off System," (in English), *Oceans-Ieee,* 2014.

[24] Y. Sang, H. Karayaka, Y. Yan, J. Z. Zhang, E. Muljadi, and Y.-H. Yu, *Energy extraction from a slider-crank wave energy converter under irregular wave conditions*. 2015, pp. 1-7.

[25] V. Arakelian, J.-P. Le Baron, and M. Mkrtchyan, "Design of Scotch yoke mechanisms with improved driving dynamics," *Proceedings of the Institution of Mechanical Engineers, Part K: Journal of Multi-body Dynamics,* vol. 230, no. 4, pp. 379-386, 2016/12/01 2015.

[26] E. Al Shami, R. Zhang, and X. Wang, "Point Absorber Wave Energy Harvesters: A Review of Recent Developments," *Energies,* vol. 12, no. 1, p. 47, 2018.

[27] W. E. Cummins, "The impulse response function and ship motions," *Symposium on Ship Theory,* vol. 9, pp. 101-109, 1962.

[28] P. Ricci, "Time-Domain Models," in *Numerical Modelling of Wave Energy Converters*, 2016, pp. 31-66.

[29] G. H. Keulegan, L. H. Carpenter, and U. S. O. o. N. Research, *Forces on Cylinders and Plates in an Oscillating Fluid*. U.S. Department of Commerce, National Bureau of Standards, 1956.

[30] G. Giorgi and J. Ringwood, *Consistency of Viscous Drag Identification Tests for Wave Energy Applications*. 2017.

[31] B. Wu, X. Wang, X. Diao, W. Peng, and Y. Zhang, "Response and conversion efficiency of two degrees of freedom wave energy device," *Ocean Engineering,* vol. 76, pp. 10-20, 2014.

[32] S. J. Illesinghe, R. Manasseh, R. Dargaville, and A. Ooi, "Idealized design parameters of Wave Energy Converters in a range of ocean wave climates," *International Journal of Marine Energy,* vol. 19, pp. 55-69, 2017.

[33] E. Al Shami, X. Wang, R. Zhang, and L. Zuo, "A parameter study and optimization of two body wave energy converters," *Renewable Energy,* vol. 131, pp. 1-13, 2019.

[34] Y. Gao, S. Shao, H. Zou, M. Tang, H. Xu, and C. Tian, "A fully floating system for a wave energy converter with direct-driven linear generator," *Energy,* vol. 95, pp. 99-109, 2016.

[35] X. Zhang, J. Yang, and L. Xiao, "Numerical Study of an Oscillating Wave Energy Converter with Nonlinear Snap-

Through Power-Take-Off Systems in Regular Waves," presented at the The Twenty-fourth International Ocean and Polar Engineering Conference, Busan, Korea, 2014/8/7/, 2014.

[36] W. B. S. t. A. Heniges, Portland, OR, 97266), "Scotch yoke engine with variable stroke and compression ratio," United States Patent Appl. 4485768, 1984. [Online]. Available: http://www.freepatentsonline.com/4485768.html.

[37] J. Pastor and Y. Liu, "Frequency and time domain modeling and power output for a heaving point absorber wave energy converter," *International Journal of Energy and Environmental Engineering*, vol. 5, no. 2-3, 2014.